A Fast Algorithm for Estimating the Parameters of a Quadratic FM Signal

Peter O'Shea

Abstract—This paper describes a fast algorithm that can be used for estimating the parameters of a quadratic frequency modulated (FM) signal. The proposed algorithm is fast in that it requires only one-dimensional (1-D) maximizations. The optimal maximum likelihood method, by contrast, requires a three-dimensional (3-D) maximization, which can only be realized with an exhaustive 3-D grid search. Asymptotic statistical results are derived for all the estimated parameters. The amplitude estimate is seen to be optimal, whereas the phase parameters are, in general, suboptimal. Of the four phase parameter esitmates, two approach optimality as the signal-to-noise ratio (SNR) tends to infinity. The other two have mean-square errors that are within 50% of the theoretical lower bounds for high SNR. Simulations are provided to support the theoretical results. Extensions to multiple components and higher order FM signals are also discussed.

Index Terms—Cubic phase function, parameter estimation, polynomial phase signals, statistical signal processing.

I. INTRODUCTION

THE noisy quadratic frequncy modulated (FM) signals considered in this paper conform to the model

$$z_r(n) = z_s(n) + z_w(n) \tag{1}$$
$$= b_0 e^{j(a_0 + a_1 n + a_2 n^2 + a_3 n^3)} + z_w(n)$$
$$-\frac{N-1}{2} \le n \le \frac{N-1}{2} \tag{2}$$

where $z_w(n)$ is complex white Gaussian noise of power, σ^2, and $\{a_0, a_1, a_2, a_3, b_0\}$ are the parameters to be estimated. N is assumed to be odd, and the sampling rate is assumed (without loss of generality) to be unity.

Quadratic FM signals arise in a number of applications. Two such applications are described in [14]. The first is passive intelligent radar surveillance, where one tries to determine whether a linear FM, quadratic FM, or other type of radar pulse is being transmitted. The second application is in the processing of echolocation signals from brown bats. These signals are multiple component quadratic FM sonar signals, with the parameters of the FM signals varying according to the activity of the bat.

Maximum likelihood (ML) estimation of the parameters of FM signals can be achieved by a simple generalization of ML estimation of the parameters of tones [1], [16]. This generaliza-

tion gives rise to the following estimators for the parameters of a quadratic FM signal:

$$(\hat{\alpha}_1, \hat{\alpha}_2, \hat{\alpha}_3)$$
$$= \arg \max_{(a_1, a_2, a_3)} \left| \sum_{n=-(N-1)/2}^{(N-1)/2} z_r(n) e^{-j(a_1 n + a_2 n^2 + a_3 n^3)} \right| \tag{3}$$

$$\hat{b}_0 = \frac{1}{N} \left| \sum_{n=-(N-1)/2}^{(N-1)/2} z_r(n) e^{-j(\hat{\alpha}_1 n + \hat{\alpha}_2 n^2 + \hat{\alpha}_3 n^3)} \right| \tag{4}$$

$$\hat{\alpha}_0 = \text{angle} \left\{ \sum_{n=-(N-1)/2}^{(N-1)/2} z_r(n) e^{-j(\hat{\alpha}_1 n + \hat{\alpha}_2 n^2 + \hat{\alpha}_3 n^3)} \right\} \tag{5}$$

where $\hat{b}_0$, $\hat{\alpha}_0$, $\hat{\alpha}_1$, $\hat{\alpha}_2$, and $\hat{\alpha}_3$ are the ML estimates of b_0, a_0, a_1, a_2, and a_3, respectively, and "argmax" denotes "the argument which maximizes."

It is clear from (3) that a three-dimensional (3-D) maximization is required to implement the ML algorithm. If the 3-D surface being maximized were convex, the maximization could be achieved very simply with gradient based techniques. The surface, however, is not, in general, convex. In particular, when there is heavy noise, there can be *many* local maxima. To implement the ML solution, therefore, one would have to do an exhaustive 3-D grid search to find the vicinity of the global maximum. Once this vicinity is found, a gradient-based Newton algorithm can be used for refinement. This type of approach is described in [1] for a linear FM signal.

A direct 3-D grid search in (3) would require $O(N^3 \log N)$ operations. To avoid this kind of multidimensional search, Djuric and Kay proposed the use of phase unwrapping and linear regression. This method is computationally very efficient and provides statistically optimal parameter estimates above about 7 dB but only for mono-component signals. The algorithms in [3]–[5], [6], and [12] are another computationally efficient alternative and can be used to obtain parameter estimates which are almost asymptotically optimal. These techniques also have the advantage that they can be used for processing multiple components [13]; a disadvantage, however, is that they involve fourth- or higher order nonlinearities, which is a fact that limits their performance below SNRs of about 0 dB. This paper presents an algorithm that is based on the CP function introduced in [9]. This function involves only second-order nonlinearities and, as a consequence, allows parameter estimation at lower SNRs.

The proposed algorithm is outlined in Section II. Asymptotic statistical results are presented in Sections III, and Section IV

presents simulations that support the theoretical results. Section V comments on multicomponent analysis, whereas Section VI discusses extensions to parameter estimation for higher order FM signals. The derivations of the first-order statistical results are provided in the appendices.

II. PARAMETER ESTIMATION

A. Preliminary Discussion

The CP function was introduced in [9] for the purposes of estimating the instantaneous frequency rate (IFR) of a signal. The latter is defined for a signal with phase $\phi(n)$ as

$$\text{IFR}(n) = \frac{d^2\phi(n)}{dn^2}. \tag{6}$$

The discrete-time CP function for an arbitrary signal $z_r(n)$ is given by

$$\text{CP}_{z_r}(n, \Omega) = \sum_{m=0}^{(N-1)/2} z_r(n+m)z_r(n-m)e^{-j\Omega m^2}. \tag{7}$$

Note that although there are only $(N+1)/2$ terms in the above summation, the incorporation of the $z_r(n+m)z_r(n-m)$ term ensures that all N samples in the data are used. The function in (7) may be thought of as having two elements. The first element is the preprocessing operation $z_r(n+m)z_r(n-m)$. The second element is the application of a bank of quadratic phase filters via the $\sum_{m=0}^{(N-1)/2}(.)e^{-j\Omega m^2}$ operator. In order to provide insight into the working of the CP function, the role of both elements are considered in the ensuing paragraphs.

The effect of the preprocessing element is to convert a third-order polynomial phase signal into one that, at any given value of time n, has only quadratic and initial phase terms. Consider, for example, the third-order polynomial phase signal in (2). When this signal is subjected to the preprocessing operation $z_r(n+m)z_r(n-m)$, the result is

$$
\begin{aligned}
&z_r(n+m)z_r(n-m) \\
&= b_0^2 e^{j2[(a_0+a_1n+a_2n^2+a_3n^3)+(a_2+3a_3n)m^2]} \\
&\quad + z_w(n-m)b_0 e^{j[(a_0+a_1(n+m)+a_2(n+m)^2+a_3(n+m)^3)]} \\
&\quad + z_w(n+m)b_0 e^{j[(a_0+a_1(n-m)+a_2(n-m)^2+a_3(n-m)^3)]} \\
&\quad + z_w(n+m)z_w(n-m).
\end{aligned} \tag{8}
$$

The right-hand side of (8) contains four terms, the first being a deterministic one, and the subsequent ones being random. For a given value of time n, the deterministic term is a constant amplitude signal, with one phase component that is quadratic in m and another invariant to m. The preprocessed signal is therefore a constant amplitude signal with "initial phase" and "quadratic phase" components embedded in random noise. The quadratic phase coefficient of the preprocessed signal is $2(a_2 + 3a_3n)$, which corresponds to the IFR of the signal.

Because the IFR of the signal is equal to the quadratic phase coefficient of the preprocessed signal, the problem of IFR estimation essentially amounts to estimation of the quadratic phase coefficient in the preprocessed signal. This estimation is the task of the second element of the CP function. The estimation is described in the next paragraph.

An obvious way to estimate a quadratic phase coefficient from a time series is to use the nonlinear least squares estimator. Given the preprocessed signal on the left-hand side of (8), the nonlinear least squares estimator for the quadratic phase coefficient (i.e., for the IFR) is

$$\hat{\text{IFR}}(n) = \arg\max_{\Omega} |CP_{z_r}(n, \Omega)|. \tag{9}$$

Thus, the IFR at any point in time can be readily obtained as the argument which maximizes the CP function magnitude.

Maximization of the CP function directly according to (9) would require $O(N^2)$ operations. This can be reduced to $O(N\log N)$ operations, however, with the use of subband decomposition techniques. That is, just as one can efficiently compute discrete Fourier transforms by using subband decomposition in the frequency domain, one can efficiently compute CP functions by the use of subband decomposition in the frequency rate (Ω) domain. In practice, one could obtain obtain a coarse estimate of the maximum with a grid search over Ω. A refined estimate could be obtained with the algorithm in [1]. A parameter estimation algorithm that uses the CP function is discussed next.

B. Overview of the Algorithm

For a noiseless quadratic FM signal, the IFR is specified by

$$\text{IFR}(n) = 2[a_2 + 3a_3n]. \tag{10}$$

From the above equation, it is clear that if the IFR is known at two different time positions, then a_2 and a_3 can be determined. For a noisy quadratic FM signal, it will not be possible to know the IFR exactly, but it will be possible to estimate it from the peak of the CP function.

Motivated by the above facts, the first step of the proposed algorithm determines IFR estimates at two different time positions by extracting peaks from the CP function. In Step 2, these two IFR estimates are then used, along with (10), to determine estimates of a_2 and a_3. The choice of the two different time positions for the IFR estimates affects the variance of the resulting a_2 and a_3 estimates. If one of the time positions is chosen to be $n = 0$, then both the a_2 and a_0 estimates will be asymptotically optimal at high SNR. (See Appendices B and D). For this reason, the suggested default setting for the time position of the first IFR estimate is $n = 0$. The suggested time position for the second IFR estimate is that which gives rise to minimum asymptotic mean-square error (MSE) for the a_3 estimate at high SNR. This value is found in Appendix B to be $n \approx 0.11N$.

Once the a_2 and a_3 parameters have been estimated, the observation can be appropriately dechirped to leave a near-linear phase component in additive noise. Conventional linear-phase techniques can then be used to estimate the remaining parameters [16]. This is what is done in Steps 4 and 5.

C. Algorithm

The specification of the fast algorithm is as follows.

Step 1) Estimate two IFRs $\hat{\Omega}_1$ and $\hat{\Omega}_2$, at times, n_1 and n_2, respectively

$$\hat{\Omega}_1 = \arg\max_{\Omega} |CP_{z_r}(n_1, \Omega)| \tag{11}$$

$$\hat{\Omega}_2 = \arg\max_{\Omega} |CP_{z_r}(n_2, \Omega)|. \tag{12}$$

(Suggested defaults for n_1 and n_2 are 0 and $0.11N$, respectively).

Step 2) Let $\hat{\mathbf{a}} = [\hat{a}_2 \ \hat{a}_3]^T$, $\hat{\mathbf{R}} = [\hat{\Omega}_1 \ \hat{\Omega}_2]^T$ and $\mathbf{X} = \begin{bmatrix} 2 & 6n_1 \\ 2 & 6n_2 \end{bmatrix}$. Then, compute $\hat{\mathbf{a}}$ (i.e., the vector of a_2 and a_3 estimates) according to

$$\hat{\mathbf{a}} = \mathbf{X}^{-1}\hat{\mathbf{R}}. \tag{13}$$

Step 3) Estimate $\hat{a}_1$ by dechirping and finding the Fourier transform peak:

$$\hat{a}_1 = \arg\max_{a_1} \left| \sum_{n=-(N-1)/2}^{(N-1)/2} z_r(n)e^{-j(a_1n+\hat{a}_2n^2+\hat{a}_3n^3)} \right|. \tag{14}$$

Step 4) Find $\hat{b}_0$ and $\hat{a}_0$ by evaluating

$$\hat{b}_0 = \left| \frac{1}{N} \sum_{n=-(N-1)/2}^{(N-1)/2} z_r(n)e^{-j(\hat{a}_1n+\hat{a}_2n^2+\hat{a}_3n^3)} \right| \tag{15}$$

$$\hat{a}_0 = \text{angle}\left[\sum_{n=-(N-1)/2}^{(N-1)/2} z_r(n)e^{-j(\hat{a}_1n+\hat{a}_2n^2+\hat{a}_3n^3)} \right]. \tag{16}$$

Note that to avoid ambiguities inherent in the the phase parameters, it is assumed that $|a_1| \leq \pi$, $|a_2| \leq \pi/N$ and that $|a_3| \leq 3\pi/2N^2$.

III. STATISTICAL PROPERTIES OF THE PARAMETER ESTIMATES

The results of a first-order statistical analysis of the parameter estimates are summarized in Table I. (The analysis itself is performed in Appendices A–D). The second column in Table I shows the ratio of the asymptotic MSE to the Cramér-Rao (CR) bound for each of the parameter estimates. From this column, it is evident that the MSEs for $\hat{a}_0$, $\hat{a}_2$, and $\hat{b}_0$ meet the CR bounds asymptotically as SNR $\rightarrow \infty$, whereas $\hat{a}_1$ and $\hat{a}_3$ have asymptotic MSEs, which are 38.5 and 45.5%, respectively, above the CR bound as SNR $\rightarrow \infty$.

It is important to note that once the estimates have been obtained with the algorithm in Section II-C, it is possible to improve the estimates with some post-processing. This post-processing could take the form of either a Newton algorithm (see [11, App. H]) or the strategy described in the last paragraph of Section VI. Note also that in Steps 2 and 3 of the algorithm, instead of using just two IFR estimates to compute $\hat{a}_2$ and $\hat{a}_3$, one could use multiple IFR estimates along with regression techniques. This would increase the accuracy of the estimates but is not recommended. Post-processing techniques are a computationally simpler option for improving the accuracy.

A. Comparison With Alternative Methods

As stated already, the optimal way to estimate the quadratic FM parameters is with the ML algorithm. This method yields statistically optimal estimates but requires a 3-D search and is computationally prohibitive. If the SNR is above 7 dB and there is only one component present, the phase unwrapping method in [7] would be the preferred parameter estimation technique. This is so because it gives optimal parameter estimates with relatively little computation. At SNRs below 7 dB, the "multilinear function methods" in [3], [4], [6], and [12], which all involve

TABLE I
THEORETICAL MSE AND CR BOUNDS FOR PARAMETER ESTIMATES

Parameter estimate	$\dfrac{\text{Asymptotic MSE}}{\text{Cramer-Rao bound}}$	Cramer-Rao bound
$\hat{a}_0$	$1 + \frac{0.278}{SNR}$	$\frac{1.125}{SNR \cdot N}$
$\hat{a}_1$	$1.385 + \frac{1.1}{SNR}$	$\frac{37.5}{SNR \cdot N^3}$
$\hat{a}_2$	$1 + \frac{1}{2SNR}$	$\frac{90}{SNR \cdot N^5}$
$\hat{a}_3$	$1.455 + \frac{1.32}{SNR}$	$\frac{1400}{SNR \cdot N^7}$
$\hat{b}_0$	1	$\frac{\sigma^2}{2N}$

only 1-D searches, are the most obvious rivals to the CP function technique. Among these methods, the higher order ambiguity function (HAF) approach is perhaps the best known [12]. MSEs for the various HAF parameter estimates can be computed from the results in [15]. For cubic phase signals, the HAF method yields greater asymptotic MSEs than the CP function method for all phase parameters at all SNRs. At high SNR, the asymptotic MSEs for the two methods are relatively close (the HAF-based MSE for the $\hat{a}_3$ parameter, for example, is about 7% higher than the CP function based one). At low SNR, however, the asymptotic MSEs for the HAF method are much greater than those of the CP function method. This is due to the fact that at low SNR the HAF-based MSEs vary approximately in proportion to SNR^{-4} (see [15, Sect. III and IV]), whereas the CP function based MSEs vary approximately in proportion to SNR^{-2}. The superior performance of the CP function at low SNR is a direct consequence of the fact that it is based on a bi-linear function, whereas the HAF method is based on a function with fourth-order nonlinearities.

Barbarossa and co-workers modified the HAF to improve its performance in the presence of noise and multiple components [3]. Three innovations were introduced. First, the "lags" in the HAF were all made distinct. Second, the HAF was symmetrised with respect to lag. Third, the HAFs were computed for multiple sets of lags and multiplied together with some appropriate scaling. As discussed in [3], these innovations introduced significant improvements with respect to noise and multiple component performance. The poor performance at low SNRs (i.e., below 0 dB), however, essentially remained. The HAFs were also extended in [2] to enable processing of signals at low SNR. This extension, however, requires a multidimensional search and is computationally daunting.

The Polynomial Wigner–Ville Distributions (PWVDs) are another multilinear function method used for analysing polynomial phase signals [6], [10]. In [4], some constraints were introduced into the PWVDs to improve noise performance. One of the main constraints imposed was that all the lags used in the PWVD should be distinct. For the method in [4], only the performance of the instantaneous frequency (i.e., the a_1 parameter) has been fully analyzed. For this parameter, the PWVD-based asymptotic MSE is marginally greater than the CP function based MSE at high SNR; at low SNR, however, the PWVD MSE is very much greater. (This is due to the fact that there are sixth-order nonlinearities in the PWVD of a quadratic FM signal).
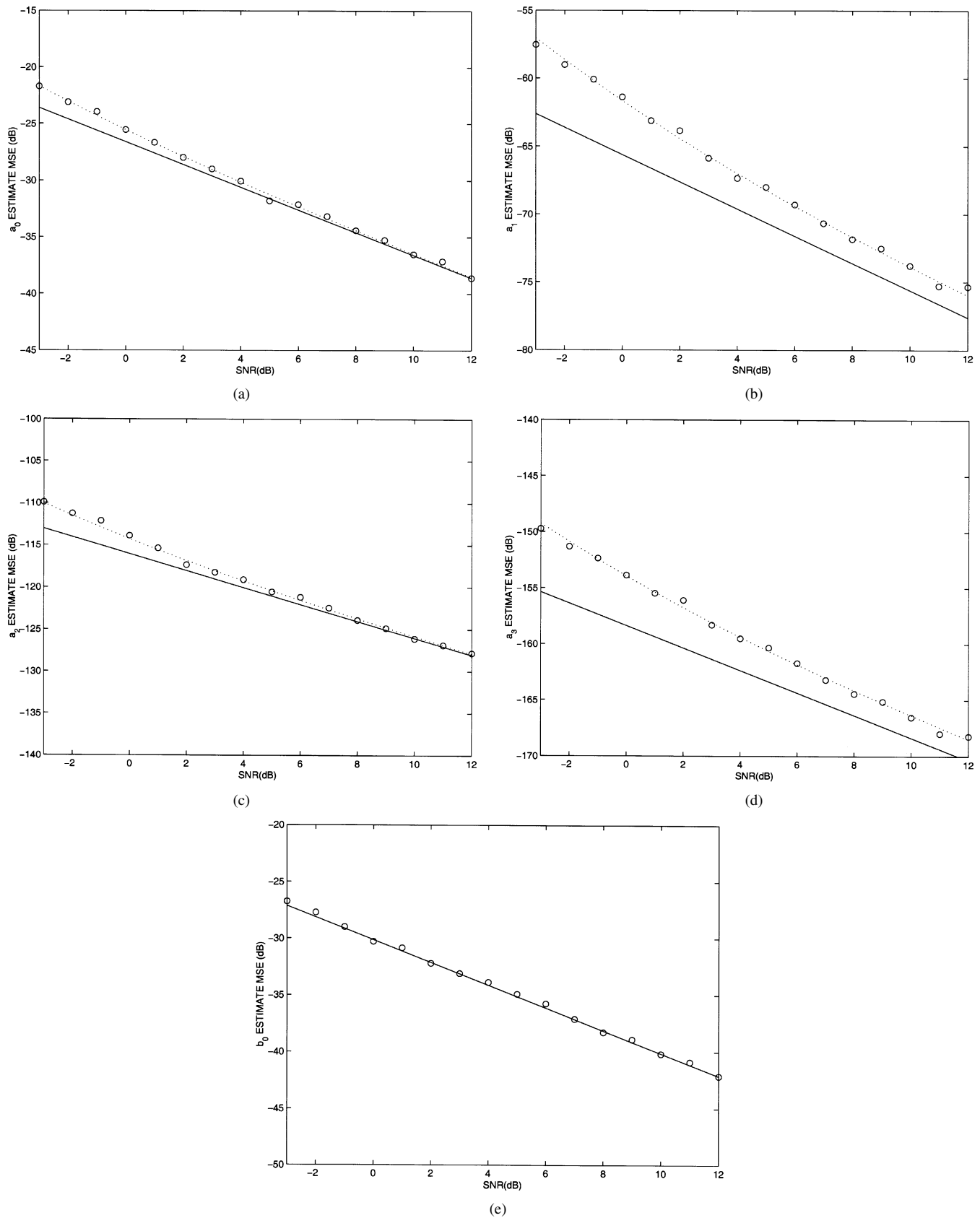
Fig. 1.   Estimate MSEs versus SNR for 515 sample signal. (Full lines are the CR bounds, dotted lines are the predicted MSEs, and circles indicate measured MSEs).

Benidir and Ouldali defined a class of general time-frequency distributions based on polynomial derivative decompositions [5]. Their definitions included generalizations of the ambiguity function and the Wigner distribution. The analysis performed

in [5] shows that the generalized class of ambiguity functions has similar theoretical performance to that of the HAFs when applied to the task of analysing polynomial phase signals. The performance of the generalized Wigner distributions was found to be poorer than that of the ambiguity function approach when applied to the same task.

IV. SIMULATIONS

The parameter estimation algorithm proposed in Section II-C was applied to a quadratic FM signal in additive, white Gaussian noise. The parameter values for the signal were chosen to be $b_0 = 1$, $a_0 = 1$, $a_1 = \pi/8$, $a_2 = 0.005$, $a_3 = 0.00001$, and $N = 515$, and the sampling rate was 1. The SNR for the signal was varied in 1-dB increments between -3 dB and $+12$ dB. For each SNR value, 500 simulations were performed, and the measured MSEs for the parameter estimates are shown in Fig. 1(a)–(e). In addition to the measured MSEs (circles), the CR bounds (full lines) and the theoretically predicted MSEs (dotted lines) are plotted. The measured MSEs are seen to all be very close to the predicted ones, and they are also in general close to the CR bounds at high SNR.

The algorithm in Section II-C was also applied to the same quadratic FM signal that was tested in [12, Sect. IV.A]. (Note, however, that 257 samples were used in the simulation here, as opposed to the 256 samples used in [12]. This minor difference was introduced because of the requirement that the CP function have an odd number of input samples). The SNR was incremented in 1–dB intervals between -6 and 15 dB, and 250 Monte Carlo simulation runs were performed for each SNR value. The $\hat{a}_3$ MSE is plotted in Fig. 2. The measured MSEs are indicated with circles, whereas the theoretical first-order asymptotic MSEs are shown as dotted lines. The straight line in the plot is the CR bound. It is evident from the plot in Fig. 2 that there is a threshold at around -2 dB. A threshold value of of ≈ -2 dB was obtained for the other phase parameter estimates as well, although the plots are not shown in the interests of brevity. Corresponding plots for the HAF-based parameter estimates are shown in [12]. The HAF algorithm is seen in [12] to threshold at a significantly higher value of SNR, i.e., at ≈ 6 dB. The difference in threshold values can largely be attributed to the differing orders of nonlinearity used in the two methods.

V. EXTENSIONS TO MULTI-COMPONENT ANALYSIS

The CP function, like the ambiguity function, is bilinear. It therefore produces "cross-terms" when multiple components are present. The cross-terms in the CP function are typically dispersed across the Ω (frequency rate) domain, analogously to the way the cross-terms are dispersed across the Doppler domain of the ambiguity function. Accordingly, the sharply peaked "auto-terms" can often be detected against the background of dispersed cross-terms in the CP function, just as they can in the ambiguity function [13].

VI. EXTENSIONS TO HIGHER ORDER FM SIGNALS

In the same way that the Wigner distribution was extended in [6] to estimate the instantaneous frequency (IF) of higher order
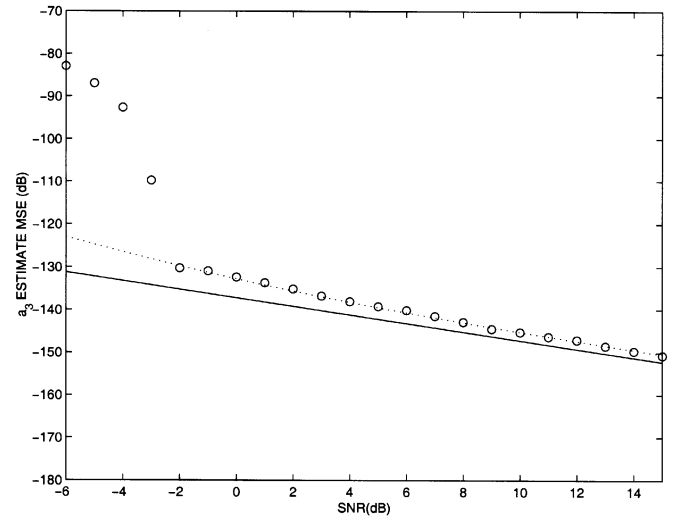

Fig. 2. $\hat{a}_3$ MSE versus SNR for 257 sample signal. (Full line is the CR bound, dotted line is the predicted first order asymptotic MSE, and circles indicate the measured MSEs).

phase signals, the CP function can be extended to estimate the instantaneous frequency rate (IFR) of higher order phase signals. These "higher order phase (HP) functions" are defined in the discrete-time domain as

$$\mathrm{HP}_{z_r}^P(n, \Omega) = \sum_m K_{z_r}^P(n, m) e^{-j\Omega m^2} \qquad (17)$$

where P is the order of the signal phase, $K_{z_r}^P(n, m) = \Pi_{i=1}^I [z_r(n + c_i m)^{k_i} z_r(n - c_i m)^{k_i}]^{r_i*}$, and $[.]^{r_i*}$ indicates conjugation of $[.]$ iff $r_i = 1$. The parameters c_i, k_i, r_i, and I are selected to yield unbiased IFR estimates for a phase polynomial of order P in much the same way that similar parameters were chosen to give unbiased estimates of the IF in [4] and [6]. With the help of these HP functions the algorithm in Section II-C can be extended to parameter estimation for FM signals of arbitrary order. A description of how to achieve this extension is provided below.

In Step 1, one finds $P - 1$ IFR estimates rather than 2. These IFR estimates can be obtained by finding the peaks of a HP function at, say, $P - 1$ equidistant points between $\approx 0.375N$ and $\approx 0.625N$. In Step 2, $\hat{\mathbf{a}}$, $\hat{\mathbf{R}}$, and $\mathbf{X}$ are all extended to be vectors of length $P - 1$. In Steps 3 and 4, the dechirped signal $z_r(n)e^{-j(\hat{a}_1 n + \hat{a}_2 n^2 + \hat{a}_3 n^3)}$ is extended to be $z_r(n)e^{-j(\hat{a}_1 n + \cdots + \hat{a}_P n^P)}$.

Finally, a postprocessing step is used to refine the phase parameter estimates to the point of optimality. This postprocessing is achieved by lowpass filtering the dechirped signal such that the cut-off frequency is about 0.05 Hz. This lowpass filtering effectively removes about 95% of the noise energy while having minimal effect on the dechirped signal energy (which is strongly concentrated around 0 Hz). The lowpass filtered signal then has its phase unwrapped, and linear regression is used to estimate its polynomial phase parameters. These estimates constitute the "fine" phase parameter estimate adjustments that are then added to the "coarse" estimates obtained in Steps 2–4. Because of the optimality of the phase unwrapping/regression approach, the resulting phase parameter estimates will be asymptotically optimal (at least above SNRs of about -3 dB).

VII. CONCLUSION

This paper has presented a fast algorithm for estimating the parameters of a noisy quadratic FM signal. The algorithm requires only 1-D maximizations, as opposed to the maximum likelihood method, which requires 3-D maximizations. A first-order statistical analysis has been presented, and it has been shown that the parameter estimates are all asymptotically optimal or near optimal at high SNR. Simulation results have been presented that show a very close adherence to the theoretically derived ones. Extensions to higher order FM signals have been discussed.

APPENDIX A
PERTURBATION ANALYSIS PRELIMINARIES

This appendix presents some key formulae that are needed for the derivations in subsequent appendices. The formulae presented herein were derived in [14].

Assume that there exists a complex valued function $g_N(\Omega)$ that depends on a real variable Ω and on an integer N. Assume further that the magnitude of $g_N(\Omega)$ has a global maximum at $\Omega = \Omega_0$ and that $g_N(\Omega)$ is perturbed by a small random function $\delta g_N(\Omega)$. This perturbation will cause the point of global maximum to be modified by an amount $\delta\Omega$. A first-order approximation for $\delta\Omega$ is [14]

$$\delta\Omega \approx -\frac{B}{A} \tag{18}$$

where

$$A = 2\mathrm{Re}\left\{ g_N(\Omega_0)\frac{\partial^2 g_N^*(\Omega_0)}{\partial\Omega^2} + \frac{\partial g_N(\Omega_0)}{\partial\Omega}\frac{\partial g_N^*(\Omega_0)}{\partial\Omega}\right\} \tag{19}$$

and

$$B = 2\mathrm{Re}\left\{ g_N(\Omega_0)\frac{\partial \delta g_N^*(\Omega_0)}{\partial\Omega} + \frac{\partial g_N(\Omega_0)}{\partial\Omega}\delta g_N^*(\Omega_0)\right\}. \tag{20}$$

The mean-squared value of $\delta\Omega$ is given by

$$E\left\{(\delta\Omega)^2\right\} \approx \frac{E\{B^2\}}{A^2} \tag{21}$$

where $E\{.\}$ signifies "the expected value."

The forumulae in (18)–(21) are used in Appendices B–D. The analysis in the subsequent appendices follows the approach used in [14]. It is assumed throughout the appendices that the estimates $\hat{a}_1$, $\hat{a}_2$, $\hat{a}_3$, $\hat{a}_0$, $\hat{b}_0$, $\hat{\Omega}_1$, and $\hat{\Omega}_2$ differ from the true parameter values by δa_1, δa_2, δa_3, δa_0, δb_0, $\delta\Omega_1$, and $\delta\Omega_2$, respectively.

APPENDIX B
MEAN-SQUARE ERROR OF THE a_3 AND a_2 ESTIMATES

Recall that $\hat{\mathbf{a}}$, which is the vector of estimates for a_3 and a_2, is obtained via (13). $\mathbf{C}_{\mathbf{a}}$, which is the covariance matrix for the parameter estimate vector $\hat{\mathbf{a}}$, is given by [8]

$$\mathbf{C}_{\mathbf{a}} = (\mathbf{X}^T\mathbf{C}_{\mathbf{R}}^{-1}\mathbf{X})^{-1} \tag{22}$$

where $\mathbf{C}_{\mathbf{R}}$ is the covariance matrix for the IFR estimate vector $\hat{\mathbf{R}}$. The element in the ith row and jth column of $\mathbf{C}_{\mathbf{R}}$ is defined by

$$\mathbf{C}_{\mathbf{R}ij} = E\{\delta\Omega_i \cdot \delta\Omega_j\}. \tag{23}$$

To find $\mathbf{C}_{\mathbf{a}}$, it is first necessary to find $\mathbf{C}_{\mathbf{R}}$. The following text is devoted to this task.

In order to apply the general formulae in Appendix A, it is useful to make the following assignment within this appendix:

$$g_N(\Omega) = CP_{z_s}(n, \Omega). \tag{24}$$

The perturbation to $g_N(\Omega)$ provided by addition of noise to $z_s(n)$ is

$$\delta g_N(\Omega) = \sum_{m=0}^{(N-1)/2-|n|} z_{ws}(n, m)e^{-j\Omega m^2} \tag{25}$$

where

$$z_{ws}(n, m) = z_s(n+m)z_w(n-m) + z_s(n-m)z_w(n+m)$$
$$+ z_w(n+m)z_w(n-m).$$

The perturbation in the position of the maximum due to the noise is $\delta\Omega$.

It is now possible to apply the formulae in (18)–(20) to derive an expression for $\delta\Omega$. A number of intermediate results are given below.

$$g_N(\Omega_0) = b_0^2 e^{j\phi(n)}\left(\frac{(N-1)}{2} - |n|\right)$$
$$\approx b_0^2 e^{j\phi(n)}\left(\frac{N}{2} - |n|\right) \tag{26}$$

$$\frac{\partial g_N(\Omega_0)}{\partial\Omega} \approx -jb_0^2 e^{j\phi(n)}\frac{(\frac{N}{2} - |n|)^3}{3} \tag{27}$$

$$\frac{\partial^2 g_N(\Omega_0)}{\partial\Omega^2} \approx -b_0^2 e^{j\phi(n)}\frac{(\frac{N}{2} - |n|)^5}{5} \tag{28}$$

$$\delta g_N(\Omega_0) \approx \sum_{m=0}^{N/2-|n|} z_{ws}(n, m)e^{-j\Omega_0 m^2} \tag{29}$$

$$\frac{\partial\delta g_N(\Omega_0)}{\partial\Omega} \approx -j\sum_{m=0}^{N/2-|n|} m^2 z_{ws}(n, m)e^{-j\Omega_0 m^2} \tag{30}$$

where $\phi(n) = 2(a_0 + a_1 n + a_2 n^2 + a_3 n^3)$.

Substituting the above results into (19) and (20) gives

$$A \approx \frac{-8b_0^4(\frac{N}{2} - |n|)^6}{45} \tag{31}$$

$$B \approx -2b_0^2\left(\frac{N}{2} - |n|\right)[\mathrm{Im}\{\Gamma\}] \tag{32}$$

where

$$\Gamma \approx e^{j\phi(n)}\sum_{m=0}^{N/2-|n|}\left(m^2 - \frac{(\frac{N}{2} - |n|)^2}{3}\right)z_{ws}^*(n, m)e^{j\Omega_0 m^2}. \tag{33}$$

Substitution of (31) and (32) into (18) gives

$$\delta\Omega \approx -\frac{45 \cdot \mathrm{Im}\{\Gamma\}}{4b_0^2(\frac{N}{2} - |n|)^5}. \tag{34}$$

Equation (34) is a general expression for the perturbation of an IFR estimate at time n. Its expected value can be shown to be zero, i.e., the bias of the IFR estimate is (to first-order approximation) zero. The covariance between two IFR estimates Ω_1 and Ω_2 at times n_1 and n_2, respectively, is

$$E\{\delta\Omega_1 \cdot \delta\Omega_2\} \approx \frac{2025 E\{\mathrm{Im}\{\Gamma_1\} \cdot \mathrm{Im}\{\Gamma_2\}\}}{16b_0^4 N^{10}d_1^5 d_2^5} \tag{35}$$

where

$$\Gamma_1 \approx e^{j\phi(n_1)}N^2 \sum_{k=0,1/N,2/N,\ldots}^{d_1}\left(k^2-\frac{d_1^2}{3}\right)z_{ws}^*(n_1,kN)e^{j\Omega_1(kN)^2}$$

(36)

$$\Gamma_2 \approx e^{j\phi(n_2)}N^2 \sum_{k=0,1/N,2/N,\ldots}^{d_2}\left(k^2-\frac{d_2^2}{3}\right)z_{ws}^*(n_2,kN)e^{j\Omega_2(kN)^2}$$

(37)

$d_1 = 1/2 - |n_1|/N$, and $d_2 = 1/2 - |n_2|/N$. $E\{\text{Im}\{\Gamma_1\} \cdot \text{Im}\{\Gamma_2\}\}$ in (35) can be simplified with some routine mathematics to

$$E\{\text{Im}\{\Gamma_1\}\cdot\text{Im}\{\Gamma_2\}\}$$
$$\approx \frac{2N^5 d_1^5 \sigma^4 \delta(n_1-n_2)}{45} + \frac{N^4 b_0^2 \sigma^2}{2}$$
$$\cdot \sum_{k=L,L+1/N,L+2/N,\ldots}^{U}\left(k^2-\frac{d_1^2}{3}\right)\left(\left(k+\frac{n_1}{N}-\frac{n_2}{N}\right)^2-\frac{d_2^2}{3}\right)$$

(38)

where $U = \min\{d_1, n_2/N - n_1/N + d_2\}$, $L = \max\{-d_1, n_2/N - n_1/N - d_2\}$, and $\delta(n_1 - n_2) = 1$ if $n_1 = n_2$ and is 0 otherwise. Substitution of (38) into (35) yields

$$E\{\delta\Omega_1 \cdot \delta\Omega_2\}$$
$$\approx \frac{45\delta(n_1-n_2)}{8(d_1 N)^5\text{SNR}^2} + \frac{2025}{32(d_1 d_2)^5 N^6\text{SNR}}$$
$$\cdot \sum_{k=0,1/N,2/N,\ldots}^{U}$$
$$\left(k^2-\frac{d_1^2}{3}\right)\left(\left(k+\frac{n_1}{N}-\frac{n_2}{N}\right)^2-\frac{d_2^2}{3}\right)$$

(39)

where SNR is defined as b_0^2/σ^2. Equation (39) can be used to determine the elements of the IFR estimate covariance matrix $\mathbf{C_R}$. The variance of an IFR estimate at time n is obtained from (39) by setting $n_1 = n_2 = n$:

$$E\{(\delta\Omega)^2\} \approx \frac{45(1+\frac{1}{2\text{SNR}})}{4(\frac{N}{2}-|n|)^5\text{SNR}}.$$

(40)

Interestingly, if the IFR is estimated at $n = 0$, the variance of this estimate is $360(1 + 1/2\text{SNR})/N^5\text{SNR}$, which is equal to the CR bound at high SNR. Furthermore, if an IFR estimate is obtained at $n = 0$ and scaled by $1/2$, an a_2 estimate is obtained, with the variance of this estimate meeting the CR bound at high SNR.

At this point, it is useful to try to determine what values of n_1 and n_2 should be used in the parameter estimation algorithm in Section II-C. Clearly, it is desirable to choose those values that give rise to estimates of a_2 and a_3 with low variances. Equations (22), (23), and (39) can be used to evaluate the variances of the a_2 and a_3 estimates as a function of n_1/N, n_2/N, and SNR. This has been done numerically using MATLAB. A choice of $n_1/N = 0$ has been found to give optimal estimates of a_2 for long data records at high SNR, regardless of the value of n_2/N. (This is in line with the discussion in the previous paragraph.) For this reason, the recommended default for n_1/N is 0. Given $n_1/N = 0$, the value of n_2/N, which gives rise to minimum variance estimates of a_3 at high SNR, has been found numerically to be ≈ 0.11. The recommended default for n_2 is therefore $0.11N$.

Note that other criteria could be used for the selection of n_1 and n_2. In particular, one could select them to minimize the average percentage deviation of the a_2 and a_3 variances from the CR bound at high SNR. If this is done, however, only a 1% reduction in average variance deviation is obtained compared with the case where n_1 and n_2 are as recommended in the previous paragraph. Moreover, as will be seen in Appendix D, the n_1 and n_2 values specified in the previous paragraph also have the advantage that they guarantee the optimality of $\hat{a}_0$ as well as $\hat{a}_2$ at high SNR. With $n_1 = 0$ and $n_2 = 0.11N$, the MSEs of a_2 and a_3 become

$$E\{(\delta a_3)^2\} \approx \frac{2038 + \frac{1844}{\text{SNR}}}{N^7\text{SNR}}$$

(41)

$$E\{(\delta a_2)^2\} \approx \frac{90(1 + \frac{1}{2\text{SNR}})}{N^5\text{SNR}}.$$

(42)

APPENDIX C
MEAN-SQUARE ERROR OF THE a_1 ESTIMATE

Once $\hat{a}_2$ and $\hat{a}_3$ have been estimated, the observation is "dechirped" so that the remaining signal is an almost linear phase component in additive noise. Then, conventional linear-phase estimation techniques can be used. An expression for the dechirped signal is

$$z_{rd}(n) = z_r(n)e^{-j(\hat{a}_3 n^3 + \hat{a}_2 n^2)}$$

(43)

$$= z_r(n)e^{-j(a_3 n^3 + \delta a_3 n^3 + a_2 n^2 + \delta a_2 n^2)}$$

(44)

$$= [z_s(n) + z_w(n)]e^{-j(a_3 n^3 + \delta a_3 n^3 + a_2 n^2 + \delta a_2 n^2)}$$

(45)

$$= [b_0 e^{j(a_0 + a_1 n)} + z_w(n)e^{-j(a_2 n^2 + a_3 n^3)}]$$
$$\cdot e^{-j(\delta a_2 n^2 + \delta a_3 n^3)}.$$

(46)

One can then make the following approximation:

$$e^{-j(\delta a_2 n^2 + \delta a_3 n^3)} \approx 1 - j\delta a_2 n^2 - j\delta a_3 n^3.$$

(47)

This approximation is possible because δa_3 is $O(N^{-7/2})$, and δa_2 is $O(N^{-5/2})$. Consequently, $\delta a_3 n^3$ and $\delta a_2 n^2$ are both order $(N^{-1/2})$ (or lower) for all n. Using the approximation in (47), an approximation for $z_{rd}(n)$ is

$$z_{rd}(n) \approx [b_0 e^{j(a_0+a_1 n)} + z_w(n)e^{-j(a_2 n + a_2 n^3)}]$$
$$\cdot (1 - j\delta a_2 n^2 - j\delta a_3 n^3).$$

(48)

For the algorithm in Section II-C, the a_1 parameter is estimated as the argument that maximizes the peak of the discrete Fourier transform of $z_{rd}(n)$. With this in mind, it is pertinent to now assign the general functions $g_N(\Omega)$ and $\delta g_N(\Omega)$ in Appendix A to be (49) and (50), shown at the top of the next page. Ω_0, which is the point of global maximum of $g_N(\Omega)$, is a_1, and the perturbation from the maximum is given by $\delta\Omega = \delta a_1$. Then, the quantities (51)–(56), shown at the bottom of the next page, can be determined. Substituting the preceding results into (19) and (20) gives

$$A \approx \frac{-b_0^2 N^4}{6}$$

(57)

$$B \approx 2N\left[\text{Im}\{\beta\} - \frac{b_0^2 \delta a_3 N^5}{80}\right]$$

(58)

$$g_N(\Omega) = \sum_{n=-(N-1)/2}^{(N-1)/2} b_0 e^{j(a_0+a_1 n)} e^{-j\Omega n} \tag{49}$$

$$\delta g_N(\Omega) = \sum_{n=-(N-1)/2}^{(N-1)/2} [z_w(n)(1 - j\delta a_2 n^2 - j\delta a_3 n^3) e^{-j(a_2 n^2 + a_2 n^3)} - b_0 e^{a_0+a_1 n}(j\delta a_2 n^2 + j\delta a_3 n^3)] e^{-j\Omega n}. \tag{50}$$

where

$$\beta \approx \sum_{n=-(N-1)/2}^{(N-1)/2} n z_s(n) z_w^*(n)(1 + j\delta a_2 n^2 + j\delta a_3 n^3). \tag{59}$$

Now

$$E\{[\text{Im}\{\beta\}]^2\} \approx \frac{\sigma^2 b_0^2 N^3}{24} \tag{60}$$

$$E\{\text{Im}\{\beta\} \cdot \delta a_3\} \approx 0, \tag{61}$$

and $E\{\delta a_3^2\}$ is given by (41). Combining (60), (61), (41), and (58) yields

$$E\{B^2\} \approx \frac{1}{6} b_0^2 N^5 \sigma^2 + \frac{1}{40^2} b_0^4 N^{12} E\{(\delta a_3)^2\} \tag{62}$$

$$= \frac{1}{6} b_0^2 N^5 \sigma^2 + \frac{1}{40^2} b_0^2 N^5 \sigma^2 \left(2038 + \frac{1844}{\text{SNR}}\right). \tag{63}$$

Finally, substituting (57) and (63) into (21) gives

$$E\{(\delta\Omega)^2\} = E\{(\delta a_1)^2\} \approx \frac{51.9 + \frac{41.5}{\text{SNR}}}{N^3 \text{SNR}}. \tag{64}$$

APPENDIX D
MEAN-SQUARE ERROR OF THE a_0 AND b_0 ESTIMATES

The derivation in this appendix follows a similar derivation in [14]. According to (15) and (16), estimation of the b_0 and a_0 parameters first requires that the observation be dechirped by

$e^{j(\hat{a}_1 n + \hat{a}_2 n^2 + \hat{a}_3 n^3)}$. An expression for the signal that has been obtained after such a dechirping is

$$z_{rd}(n) \approx b_0 e^{ja_0}[1 + b_0^{-2} z_s^*(n) z_w(n)] \cdot (1 - j\delta a_1 n - j\delta a_2 n^2 - j\delta a_3 n^3). \tag{65}$$

Now, the expression in (15) for $\hat{b}_0$ can be re-expressed as

$$\hat{b}_0 = e^{\text{Re}[\log(\lambda)]} \tag{66}$$

where

$$\lambda = \frac{1}{N} \sum_{n=-(N-1)/2}^{+(N-1)/2} z_{rd}(n). \tag{67}$$

Then, one can write

$$\text{Re}[\log(\lambda)] = \log(\hat{b}_0). \tag{68}$$

Using (65) and (67), $\log(\lambda)$ can be approximated as (69) and (70), shown at the bottom of the page. Then

$$\text{Re}\{\log(\lambda)\} \approx \log(b_0) + \text{Re}\left[\frac{1}{b_0^2 N} \sum_{-(N-1)/2}^{(N-1)/2} z_s^*(n) z_w(n)\right]. \tag{71}$$

Using (71) and (68) leads to

$$\log[\hat{b}_0] \approx \log(b_0) + \text{Re}\left[\frac{1}{b_0^2 N} \sum_{-(N-1)/2}^{(N-1)/2} z_s^*(n) z_w(n)\right]. \tag{72}$$

$$g_N(\Omega_0) \approx b_0 e^{ja_0} N \tag{51}$$

$$\frac{\partial g_N(\Omega_0)}{\partial \Omega} \approx 0 \tag{52}$$

$$\frac{\partial^2 g_N(\Omega_0)}{\partial \Omega^2} \approx -b_0 e^{ja_0} \frac{N^3}{12} \tag{53}$$

$$\delta g_N(\Omega_0) \approx \sum_{n=-(N-1)/2}^{(N-1)/2} [z_w(n)(1 - j\delta a_2 n^2 - j\delta a_3 n^3) e^{-j(a_2 n^2 + a_2 n^3)} - b_0 e^{j(a_0+a_1 n)}(j\delta a_2 n^2 + j\delta a_3 n^3)] e^{-ja_1 n} \tag{54}$$

$$\approx \frac{e^{ja_0}}{b_0} \sum_{n=-(N-1)/2}^{(N-1)/2} [z_w(n)(1 - j\delta a_2 n^2 - j\delta a_3 n^3) z_s^*(n)] - j e^{ja_0} b_0 \frac{1}{24} \delta a_2 N^3 \tag{55}$$

$$\frac{\partial \delta g_N(\Omega_0)}{\partial \Omega} \approx \frac{-e^{ja_0}}{b_0} \sum_{n=-(N-1)/2}^{(N-1)/2} jn z_w(n)(1 - j\delta a_2 n^2 - j\delta a_3 n^3) z_s^*(n) - b_0 e^{ja_0} \frac{\delta a_3 N^5}{80}. \tag{56}$$

$$\log(\lambda) \approx \log\left[\frac{b_0 e^{ja_0}}{N} \sum_{-(N-1)/2}^{(N-1)/2} \left(1 + \frac{1}{b_0^2} z_s^*(n) z_w(n)\right)(1 - j\delta a_1 n - j\delta a_2 n^2 - j\delta a_3 n^3)\right] \tag{69}$$

$$\approx \log(b_0) + ja_0 + \frac{1}{b_0^2 N} \sum_{-(N-1)/2}^{(N-1)/2} z_s^*(n) z_w(n) - j\frac{1}{12}\delta a_2 N^2. \tag{70}$$

In addition, since $\log[\hat{b}_0] = \log(b_0(1 + \delta b_0/b_0)) \approx \log(b_0) + \delta b_0/b_0$, then

$$\delta b_0 \approx \frac{1}{Nb_0}\mathrm{Re}\left[\sum_{-(N-1)/2}^{(N-1)/2} z_s^*(n)z_w(n)\right]. \qquad (73)$$

The mean squared error (MSE) of the amplitude error b_0 is then

$$\mathrm{MSE}\{\delta b_0\}$$

$$\approx \frac{1}{2N^2 b_0^2}\cdot E\left\{\left|\sum_{-(N-1)/2}^{(N-1)/2} z_s^*(n)z_w(n)\right|^2\right\} \qquad (74)$$

$$\approx \frac{\sigma^2}{2N}. \qquad (75)$$

Now, the expression for the a_0 estimate in (16) can be rewritten as $\hat{a}_0 = \mathrm{Im}[\log(\lambda)]$. Then, using (70), it is evident that

$$\hat{a}_0 = \mathrm{Im}[\log(\lambda)] \qquad (76)$$

$$\approx a_0 + \frac{1}{b_0^2 N}\mathrm{Im}\left\{\sum_{-(N-1)/2}^{(N-1)/2} z_s^*(n)z_w(n)\right\}$$

$$- \frac{1}{12}\delta a_2 N^2 \qquad (77)$$

$$\approx a_0 + \epsilon - \frac{1}{12}\delta a_2 N^2 \qquad (78)$$

where

$$\epsilon = \frac{1}{b_0^2 N}\mathrm{Im}\left\{\sum_{-(N-1)/2}^{(N-1)/2} z_s^*(n)z_w(n)\right\}. \qquad (79)$$

From (78), it can be deduced that the mean-square error of δa_0 is

$$E\left\{(\delta a_0)^2\right\} \approx E\left\{\epsilon^2\right\} + \frac{1}{144}E\left\{(\delta a_2)^2\right\}N^4$$

$$- 2E\left\{\epsilon \cdot \frac{1}{12}\delta a_2 N^2\right\}. \qquad (80)$$

An expression for $E\left\{(\delta a_2)^2\right\}$ was derived in Appendix B. The moments involving ϵ are

$$E\left\{\epsilon^2\right\} \approx \frac{1}{2\cdot\mathrm{SNR}\cdot N} \qquad (81)$$

$$E\left\{\epsilon \cdot \frac{1}{12}\delta a_2 N^2\right\} \approx 0. \qquad (82)$$

Substituting these results into (80) gives

$$E\left\{(\delta a_0)^2\right\} \approx \frac{1.125 + \frac{0.3125}{\mathrm{SNR}}}{\mathrm{SNR}\cdot N}. \qquad (83)$$

REFERENCES

[1] T. Abotzoglou, "Fast maximum likelihood joint estimation of frequency and frequency rate," *IEEE Trans. Acoust., Speech, Signal Processing*, vol. AES-22, pp. 708–715, 1986.
[2] S. Barbarossa and V. Petrone, "Analysis of polynomial phase signals by an integrated generalized ambiguity function," *IEEE Trans. Signal Processing*, vol. 47, pp. 316–327, Feb. 1997.
[3] S. Barbarossa, A. Scaglione, and G. Giannakis, "Product high-order ambiguity function for mulit-component polynomial phase signal modeling," *IEEE Trans. Signal Processing*, pp. 691–708, Mar. 1998.
[4] B. Barkat and B. Boashash, "Design of higher-order polynomial Wigner-Ville distributions," *IEEE Trans. Signal Processing*, vol. 47, pp. 2608–2611, Sept. 1999.
[5] M. Benidir and A. Ouldali, "Polynomial phase signal analysis based on the polynomial derivatives decompositions," *IEEE Trans. Signal Processing*, vol. 47, pp. 1954–1965, July 1999.
[6] B. Boashash and P. O'Shea, "Polynomial Wigner-Ville distributions & their relationship to time-varying higher order spectra," *IEEE Trans. Signal Processing*, vol. 42, pp. 216–220, Jan. 1994.
[7] P. Djuric and S. Kay, "Parameter estimation of chirp signals," *IEEE Trans. Signal Processing*, vol. 38, pp. 2118–2126, Dec. 1990.
[8] S. Kay, *Modern Spectrum Estimation*. Englewood Cliffs, NJ: Prentice-Hall, 1988.
[9] P. O'Shea, "A new technique for estimating instantaneous frequency rate," *IEEE Signal Processing Lett.*, vol. 9, pp. 251–252, Aug. 2002.
[10] ——, "Detection and estimation methods for non-stationary signals," Ph.D. dissertation, Univ. Queensland, Brisbane, Australia, 1991.
[11] S. Peleg, "Estimation and detection with the discrete polynomial phase transform," Ph.D. dissertation, Univ. California, Davis, 1993.
[12] S. Peleg and B. Friedlander, "The discrete polynomial phase transform," *IEEE Trans. Signal Processing*, vol. 43, pp. 1901–1914, Aug. 1995.
[13] ——, "Multicomponent signal analysis using the polynomial phase transform," *IEEE Trans. Aerosp. Electron. Syst.*, vol. 32, pp. 378–386, Jan. 1996.
[14] S. Peleg and B. Porat, "Linear FM signal parameter estimation from discrete-time observations," *IEEE Trans. Aerosp. Electron. Syst.*, vol. 27, pp. 607–614, July 1991.
[15] B. Porat and B. Friedlander, "Asymptotic statistical analysis of the higher order ambiguity function for parameter estimation of the polynomial phase signal," *IEEE Trans. Inform Theory*, vol. 42, pp. 995–1001, May 1996.
[16] D. C. Rife and R. R. Boorstyn, "Single tone parameter estimation from discrete-time observations," *IEEE Trans. Inform. Theory*, vol. IT-20, no. 5, pp. 591–598, 1974.

Peter O'Shea received the B.E, Dip.Ed., and Ph.D degrees in 1978, 1983, and 1991, respectively, all from the University of Queensland, Brisbane, Australia.

He was an engineer at the Overseas Telecommunications Commission for three years, at University of Queensland's Department of Electrical Engineering for four years, and then at the Queensland University of Technology (QUT), Brisbane, School of Electrical and Electronic Systems Engineering for three yearsa before moving to the School of Electrical and Computer Systems Engineering, RMIT University, Melbourne, Australia. He spent seven years at RMIT. He has recently re-joined the staff of the School of Electrical and Electronic Systems Engineering at QUT. His interests are in signal processing for communications and power systems, reconfigurable computing, and the use of multimedia in engineering education.

Dr. O'Shea received the Faculty of Engineering and President's awards for Student Centred Teaching from RMIT University.